Low-mass e^+e^- pair production in 158 A GeV Pb-Au collisions at the CERN SPS, its dependence on multiplicity and transverse momentum *

G. Agakichiev[a], R. Baur[b], P. Braun-Munzinger[c], F. Ceretto[d], A. Drees[b†], S. Esumi[b], U. Faschingbauer[b,d], Z. Fraenkel[e], Ch. Fuchs[d], E. Gatti[f], P. Glässel[b], C. P. de los Heros[e], P. Holl[g], Ch. Jung[b], B. Lenkeit[b], M. Messer[b], Y. Panebrattsev[a], A. Pfeiffer[b], J. Rak[d], I. Ravinovich[e], S. Razin[a], P. Rehak[g], M. Richter[b], M. Sampietro[f], N. Saveljic[a], J. Schukraft[h], S. Shimansky[a], W. Seipp[b], E. Socol[e], H. J. Specht[b], J. Stachel[b], G. Tel-Zur[e], I. Tserruya[e], T. Ullrich[b], C. Voigt[b], C. Weber[b], J. P. Wessels[b], T. Wienold[b], J. P. Wurm[d], V. Yurevich[a]

(CERES Collaboration)

[a] *JINR, Dubna, Russia*

[b] *Universität Heidelberg, Germany*

[c] *GSI, Darmstadt, Germany*

[d] *Max-Planck-Institut für Kernphysik, Heidelberg, Germany*

[e] *Weizmann Institute of Science, Rehovot, Israel*

[f] *Politecnico di Milano, Italy*

[g] *Brookhaven National Laboratory, Upton, USA*

[h] *CERN, Geneva, Switzerland*

(November 2, 2013)

Abstract

We report a measurement of low-mass electron pairs observed in 158 GeV/nucleon Pb-Au collisions. The pair yield integrated over the range of invariant masses $0.2 \leq m \leq 2.0$ GeV/c^2 is enhanced by a factor of 3.5 ± 0.4 (stat) $\pm$ 0.9 (syst) over the expectation from neutral meson decays. As observed previously in S-Au collisions, the enhancement is most pronounced in the invariant-mass region 300-700 MeV/c^2. For Pb-Au we find evidence for a strong increase of the enhancement with centrality. In addition, we show that the enhancement covers a wide range in transverse momentum, but is largest at the lowest observed $p_\perp$.

†Now at State University New York at Stony Brook

*Doctoral Thesis of C. Voigt.

Three experiments at the CERN Super-Proton Synchrotron (HELIOS-3 [1], NA38 [2] and CERES/NA45 [3]) have observed significantly more dileptons from central collisions of 200 GeV/nucleon sulfur beams with heavy targets than is expected from 'conventional sources' [4,5]. The enhancement is most conspicuous for electron pairs in the region of invariant masses from 300 to 700 MeV/c^2 measured close to midrapidity [3]. The comparison to expectations from conventional sources rests on a simultaneous study of neutral meson and e^+e^- pair production in 450 GeV p–Be and p–Au [6,7] where it was demonstrated that the measured e^+e^- pair mass spectra are very well described in shape as well as absolute yield by the direct and Dalitz decays of neutral mesons. For S-Au, the hadronic sources were scaled proportional to charged-particle multiplicity. The observations stimulated an intense discussion of the processes involved in the emission of low-mass dileptons from dense and hot hadronic matter. The extra strength obtained from $\pi\pi$-annihilation and other scattering processes is not sufficient to explain the dilepton data [8–11]. Most theoretical approaches therefore have focused on the way vector mesons may change inside the dense and hot medium. Dropping meson masses, derived from theoretical arguments related to chiral symmetry restoration [12,13] turned out as a suitable ingredient that creates sufficient strength below the ρ/ω resonance. This allowed to describe simultaneously the sulfur data from CERES and HELIOS-3 [8,9]. Presently, more conventional approaches in which in-medium modifications of the meson properties are related to hadronic rescattering processes that broaden the strength rather than shift it downwards also give good agreement with existing data [10].

In view of the highly complex physics processes in dense hadron matter it is clear that more and better data are mandatory. In this letter, we present first results for the 158 GeV/nucleon Pb-Au collisions in order to (i) demonstrate that the low-mass dielectron enhancement is also present in the lead data, (ii) provide first evidence for a statistically significant stronger-than-linear dependence of the pair yield on charged-particle multiplicity, and (iii) show the dependence of the pair yield on the transverse momentum $p_\perp$. Part of the data were already presented in preliminary form [14].

CERES is an experiment especially designed for the detection and measurement of low mass electron positron pairs. Electron pairs are reconstructed from invariant masses of a few tens of MeV/c^2 up to 2 GeV/c^2 in the pseudorapidity region $2.1 < \eta < 2.65$. Originally, the setup was optimized to investigate p- and S-induced collisions, providing electron identification and tracking by two ring-imaging Cherenkov counters (RICH-1, RICH-2). One is situated before and one after an axially symmetric magnetic field confined to a narrow region between the two radiators [15]. While the experiment was used successfully to measure e^+e^- production in p-Be, p-Au [7] and S-Au [3] collisions, an upgrade was necessary to cope with the high-multiplicity environment in Pb-Au collisions. With more than 300 charged particles emitted into the CERES acceptance in a central collision, the pattern recognition based solely on the RICH detectors breaks down. Therefore, the spectrometer was supplemented by charged-particle tracking devices, namely a closely-spaced doublet of silicon drift detectors (SDD) downstream of the target and before RICH-1, and a multiwire proportional chamber with pad readout (PadC) downstream of RICH-2. The information from these detectors combined with the RICH data restores the necessary reconstruction efficiency. In addition, they provide extra background rejection and improve the momentum resolution and, hence, the invariant-mass resolution of the spectrometer. The rate capability

of the data acquisition system was improved by a factor of four allowing the collection of more than 500 events per 5s burst of the SPS. With this setup $16{\cdot}10^6$ events from Pb-Au collisions were recorded during a 10 day running period in the fall of 1995. The events were selected requiring a minimum amplitude in a scintillator array downstream of the spectrometer. The trigger covers a large range of charged-particle multiplicities in order to study the impact parameter dependence.

In the off-line track reconstruction, first the event vertex is reconstructed from more than a hundred particle trajectories traversing both SDDs. Independently, Cherenkov ring candidates are reconstructed according to a pattern recognition algorithm [15] in both RICH detectors. Each track segment from the vertex to the SDDs is then extrapolated into RICH-1, where its angular coordinates are compared to those of the centers of all ring candidates found. Approximately 10% of all SDD trajectories match to a ring center within a 5 mrad window, and are marked as potential electron track segments. Many of these do not originate from electrons or positrons since a large fraction of the ring candidates are accidental combinations of photon hits. These fake tracks are removed in subsequent steps of the analysis. All segments are further extrapolated through the magnetic field into the PadC. Because the momentum and therefore the deflection in the magnetic field is not known at this stage of the analysis, every hit in the PadC within a certain area has to be combined with the track segment constructed so far. The azimuthal size of this area is defined by a cut on transverse momentum, $p_\perp \geq 50$ MeV/c, its size in polar angle θ by the combined $\pm$ 3 σ-widths of detector resolutions, multiple scattering and higher order effects, which amounted to ≈ 1.8 mrad. Within these boundaries more than two hits are found on average, but only the small fraction which matches to a Cherenkov ring in RICH-2 is accepted. Finally, cuts on the quality of Cherenkov rings as well as on the track match between individual detectors reduce the amount of fake tracks to a level below 1%. Possible ambiguities in the tracking are removed by requiring the best match in radial direction between all the detectors. This scheme leads to the reconstruction of unique e^+e^- tracks, with one exception: electron and positron tracks originating from photon conversions or Dalitz pairs of small opening angle are allowed to share the same ring in RICH-1 since the double-ring resolution in RICH-1 is insufficient to resolve all of these so-called V-tracks. The momentum is determined combining all measurements along the track, three space points and two angles, each weighted according to detector resolution and multiple scattering. The relative momentum resolution obtained is $(\sigma_p/p)^2 = 0.0012 + 0.001p^2$ (p in GeV/c), better by nearly 50% at high momenta compared to the original setup.

Most tracks belong to pairs from photon conversions and π^0 Dalitz decays, characterized by small opening angles (close pairs) and low invariant masses. In order to reduce for each track the number of possible combinations, tracks from unambiguously identified close pairs are taken out of the sample. V-tracks are removed. About 90% of all pairs with opening angles smaller than 50 mrad and invariant masses below 150 MeV/c^2 result from Dalitz decays. They are kept in the sample but marked as assigned tracks, and hence not combined with others. For a significant fraction of close pairs only one track is reconstructed due to the finite reconstruction efficiency and acceptance. Its combination with other tracks creates the combinatorial pair background.

The central problem of the analysis is to recognize and reject as many of the partially

reconstructed conversions and Dalitz decays as possible. An important kinematic characteristic of conversions and Dalitz decays is the softness of the $p_\perp$ spectra of electrons and positrons compared to those for pairs with masses above 0.2 GeV/c^2. This allows for a drastic suppression of background tracks by requiring $p_\perp \geq 200$ MeV/c for each track. Another characteristic is the small opening angle, and since there is no magnetic field upstream of and within RICH-1, the opening angle of a pair remains unchanged through half of the setup. Thus a pair with small opening angle can be identified even if the trajectory of one of its tracks is incompletely measured. Depending on the size of the pair opening angle, different information is exploited. (i) Opening angles smaller than the double hit resolution of the SDD system (< 5 mrad) result in unresolved double tracks which deposit in both SDDs, on average, twice the energy loss of one particle. A two-dimensional cut on both dE/dx measurements strongly rejects such very close pairs without impairing reconstruction efficiency by more than a few percent. (ii) For opening angles larger than 5 mrad but below 12 mrad – the double ring resolution of the RICH-1 – most double tracks will be resolved in the SDDs, but they match to only one ring in RICH-1. Imposing an upper limit on the number of Cherenkov photons removes a large fraction of tracks corresponding to these pairs. (iii) Pairs with even larger opening angles are recognized if the second Cherenkov ring in RICH-1 and a corresponding trajectory in the SDD system are found. Tracks are rejected if the neighboring ring is closer than 50 mrad. In order to simplify the comparison to the S-Au analysis, we require the pair opening angle to be larger than 35 mrad. The combined effect of all rejection cuts improves the signal-to-background ratio by more than one order of magnitude.

The remaining combinatorial background in the e^+e^- sample is estimated by the number of like sign pairs. In order to calculate the pair signal S, the like sign contribution is subtracted from the e^+e^--sample such that $S = N_{+-} - 2\sqrt{N_{++}N_{--}}$. The mass distribution of unlike-sign and of the geometrical mean of like-sign pairs is shown in Fig. 1. In order to reduce statistical bin-to-bin fluctuations, the like-sign spectra were smoothed before subtraction. The smoothed pair background is created from tracks which are generated randomly according to the measured $p_\perp$, θ and ϕ distributions of tracks from like-sign pairs. By this technique, an excellent description of the like-sign mass, $p_\perp$ and opening angle distributions is achieved in all observed phase space selections.

The final sample contains 1038 ± 55 reconstructed e^+e^- pairs for invariant masses below 0.2 GeV/c^2 at a signal-to-background ratio of 1.05. For masses above 0.2 GeV/c^2 we find 5834 e^+e^-, 2494 e^+e^+, and 2696 e^-e^- pairs resulting in a net signal of 648 ± 105 pairs with a signal-to-background ratio of 1/8. The difference spectrum turns out to be stable in shape and yield with respect to details of the rejection cuts, as elaborated below.

The resulting mass spectrum of pairs has to be corrected for efficiency. The fraction of pairs which are reconstructed by our procedure is estimated using a Monte-Carlo simulation in which individual lepton pairs from neutral meson decays are generated (see below for more details). The full detector response is modeled with a GEANT-based [16] simulation and the specific detector properties. Lacking precise knowledge of how to generate complete events – in particular beam environment background – these simulated pairs are embedded into real data and are then analyzed using the standard software chain. On average about 50% of the tracks are reconstructed, implying a pair reconstruction efficiency of about 25%.

The background rejection cuts discussed above, however, reduce the number of reconstructed pairs to about 12%. The reconstruction efficiency also depends on the multiplicity in the event. It decreases considerably with increasing multiplicity from 16% for $dN_{ch}/d\eta$=120 to 9% for $dN_{ch}/d\eta$=350. No significant mass dependence of the efficiency is observed.

Fig. 2 shows the resulting invariant-mass spectrum of e^+e^- pairs. The event sample corresponds to the most central 35% of the geometrical cross section with an average charged multiplicity of $\langle dN_{ch}/d\eta \rangle = 220$ in our acceptance[1]. The pair density has been normalized to $\langle dN_{ch}/d\eta \rangle$ measured in the pseudorapidity region 2.1 to 2.65 by the silicon drift detectors. The statistical errors of the data are shown as bars whereas systematic errors are given separately as brackets. The systematic errors contain contributions from the background smoothing procedure, the uncertainties of the absolute background level, the reconstruction efficiency and the determination of the average multiplicity. They add to 25-40%, depending on mass, and are strongly correlated for different mass bins.

Due to the small signal-to-background ratio, the background subtraction is of crucial importance for the reliability of the signal. In our case, this is even more so, because within the present statistics the spectral shape of signal and background are not very different for masses above 200 MeV, thus raising the question whether the combinatorial background has been subtracted correctly. For each analysis cut, background rejection power and pair reconstruction efficiency have been optimized simultaneously for four bins of charged-particle multiplicity. The efficiency is obtained from the Monte-Carlo simulation, while the rejection power is judged from the measured like-sign pair background. The size of the signal itself was disregarded in the optimization procedure in order to avoid the risk of being mislead by statistical fluctuations in the data. We have performed two checks on the stability of our results: (i) All background rejection cuts have been simultaneously varied, without bias and at random within windows of $\approx \pm 15\%$ around the optimum values. Several hundred cut settings were investigated. After efficiency correction the result remained within the systematic errors quoted. (ii) The analysis was repeated using different combinations of cuts, once without applying the final background rejection cuts and in a second test with very much relaxed quality cuts in the tracking but including the final rejection cuts. The signal-to-background ratio deteriorated from 1/8 to 1/25 and 1/30, respectively. Although the background level is larger by a factor of more than $\sim$3, the final result remained stable within statistical errors.

The data are compared to the expected e^+e^- pair yield from decays of π^0, η, η', ρ, ω, and ϕ, in line with ref. [6,7] where a more detailed description can be found. The relative meson abundances are assumed to be independent of the collision system. Their yield is scaled proportional to $\langle dN_{ch}/dy \rangle$. The rapidity distribution for pions is deduced from a Gaussian fit to measured data [17], for heavier mesons the width of the rapidity distribution is scaled using the maximum possible rapidity for a given particle species of mass m as $y_{max}(m)/y_{max}(\pi)$. Similarly, the pion $p_\perp$ distribution is generated according to a fit of data from various experiments [17–19]. Higher mass mesons are modeled according to measured

[1] In an earlier presentation of a preliminary analysis the charged-particle density used was higher by 15% due to an overestimate of a pileup correction [14].

kaon $p_\perp$ distributions, assuming $m_\perp$ scaling [2]. Finally, the laboratory momenta of dileptons produced in decays of these mesons are convoluted with the experimental resolution and acceptance. The generated events were analyzed using the same $p_\perp$ and opening-angle cuts as in the data analysis.

The invariant-mass spectrum from meson decays is in good agreement with data below 200 MeV/c^2 where the expected contribution is dominated by π^0 Dalitz decays. Above 200 MeV/c^2, the measured pair yield is clearly enhanced, most pronounced in the region from 300 to 700 MeV/c^2. Integrating over this mass range, the combined yield of the 'hadronic cocktail' is exceeded by a factor of 5.8 ± 0.8(stat) $\pm$ 1.5 (syst). The enhancement, however, extends up to the highest observed masses. In the larger interval $0.2 \leq m \leq 2.0$ GeV/c^2, the enhancement factor is still 3.5 $\pm$ 0.4 (stat) $\pm$ 0.9 (syst). The shape expected from the generator spectrum has little correspondence to the data. In particular, the resonance structures of ρ/ω and ϕ are not visible albeit indicated by a sharply dropping yield on the high-mass side. The detection of the ρ/ω peak clearly is within the capabilities of the mass resolution of $\sigma_m/m_{\rho/\omega} \sim 8\%$, as can be seen from the solid line in Fig. 2. In contrast, the peak was observed as a prominent feature in the invariant-mass spectra of e^+e^- pairs from p–Be and p–Au collisions, with a mass resolution of only 11% at $m_{\rho/\omega}$ [7].

The large impact parameter range covered by the data allows for a study of the multiplicity dependence of the pair yield. If all pairs were originating from decays of produced hadrons as scaled up from p–A collisions, the pair yield should be proportional to charged-particle multiplicity, as does the yield of produced hadrons in the generator. Compared to this well-defined reference, any stronger-than linear dependence of the e^+e^- yield on N_{ch} indicates that pairs evolve from higher generations of hadrons or partons formed inside the firecylinder, by any thermal hadro-chemical reaction in general, or pion annihilation $\pi\pi \rightarrow \rho$ followed by virtual photon radiation, in particular.

The sample is divided into four subsets in charged-particle multiplicity containing about equal numbers of events. Fig. 3 gives the electron pair density normalized to charged-particle density integrated over the mass range $0.2 \leq m \leq 2$ GeV/c^2 for each of the multiplicity bins. Also shown are the CERES results for the lighter collision systems p-Be and p-Au [7]. The reference assumption is illustrated by the horizontal line in the figure, the normalized pair density would remain constant. A significant rise of the normalized pair yield is observed, such that the dilepton yield grows faster than linear with multiplicity. This is illustrated by the dashed line which shows a linear fit of the Pb-Au data. With an error of ~ 0.2 the perfect agreement of the intercept at $\langle dN_{ch}/dy \rangle = 0$ with the yield observed in p-induced collisions and the expectation from hadron decays seems fortuitous. By applying a non-parametric statistical test, the hypothesis of a linear scaling of the dilepton yield from p-Be to central Pb-Au can be excluded with a 94% confidence level.

The statistics of the present data sample is sufficient to extract pair transverse-

[2] Due to our relatively low $p_\perp$ cut of 200 MeV/c only the contribution of π° and η is influenced by the assumed $p_\perp$ distribution. Tracks from higher-mass mesons pass the $p_\perp$ cut rather independent of the assumed distribution. Therefore, including for example an increase of the slope parameter with particle mass as observed in central Pb-induced collisions [17,18], would not alter our prediction of the e^+e^- contribution from meson decays.

momentum spectra for three invariant-mass regions. The experimental data are plotted in Fig. 4. One should note that the single-track $p_\perp$-cut strongly affects the $p_\perp$ distribution for masses below 400 MeV/c^2, dominating the shape of the pair $p_\perp$ spectra at low $p_\perp$. The generator curves shown are folded with momentum resolution and normalized as was discussed above. For masses below 200 MeV/c^2 the $p_\perp$ distribution agrees with the prediction for π^0 Dalitz decays (left panel). For higher masses, the enhancement is visible over the entire $p_\perp$ range but it significantly increases towards very low $p_\perp$ for m$\geq$ 200 MeV/c^2.

In summary, we have presented first results of e^+e^- pair production in Pb-Au collisions. Above masses of 0.2 GeV/c^2 the continuum is enhanced compared to the yield expected from neutral meson decays by scaling from p-induced reactions. This result corroborates previous findings with sulfur beam where a similar enhancement of the continuum was found for $\mu^+\mu^-$ [1] and e^+e^- [3] pairs. For central Pb-Au and S-Au collisions the spectral shape and magnitude of the e^+e^- pair enhancement are similar. The larger statistics available for Pb-Au collisions allowed to extend the mass range up to 2 GeV/c^2. We have found evidence for a strong increase of the pair excess with centrality as expected for thermal radiation. First data on $p_\perp$-spectra show that the yield is amplified over the entire range, but it is strongest at the lowest $p_\perp$ measured.

The CERES collaboration acknowledges the good performance of the CERN PS and SPS accelerators. We are grateful for support by the German BMBF, the U.S. DoE, the MINERVA Foundation, the German-Israeli Foundation for Scientific Research and Development, and the Israeli Science Foundation.

REFERENCES

[1] M. Masera et al. (HELIOS/3-Collaboration), Nucl. Phys. A590 (1995) 93c.
[2] C. Lourenço, Doctoral Thesis, Universidade Tecnica de Lisboa (1995).
[3] G. Agakichiev et al. (CERES-Collaboration), Phys. Rev. Lett. 75 1272 (1995).
[4] I. Tserruya, Nucl. Phys. A590 (1995) 127c.
[5] A. Drees, Nucl. Phys. A610 (1996) 536c; Nucl. Phys. A630 (1998) 449c.
[6] G. Agakichiev et al. (CERES-Collaboration), Neutral meson production in p-Be and p-Au collisions at 450 GeV beam energy, Z. Phys. C. (in print).
[7] G. Agakichiev et al. (CERES-Collaboration), Systematic study of low-mass electron pair production in p-Be and p-Au collisions at 450 GeV/c, Z. Phys. C. (in print).
[8] G. Q. Li, C. M. Ko, and G. Brown, Phys. Rev. Lett. 75 (1995) 4007; Nucl. Phys. A606 (1996) 568.
[9] W. Cassing, W. Ehehalt, and C. M. Ko, Phys. Lett. B363 (1995) 35; W. Cassing, W. Ehehalt, and I.Králik, Phys. Lett. B377 (1996) 5.
[10] R. Rapp, G. Chanfray, and J. Wambach, Phys. Rev. Lett. 76 (1996) 368; Nucl. Phys. A617 (1997) 472.
[11] D. K. Srivastava, B. Sinha, and C. Gale, Phys. Rev. C53 (1996) R567; J. Sollfrank et al., Phys. Rev. C55 (1997) 392; C. M. Hung and E. V. Shuryak, Phys. Rev. C56 (1997) 453; V. Koch and C. Song, Phys. Rev. C54 (1996) 1903; R. Baier, M. Dirks, and K. Redlich, Phys. Rev. D55 (1996) 4344; J. Murray, W. Bauer, and K. Haglin, hep-ph/9611328, to be published; L. Winckelmann et al., Nucl. Phys. A610 (1996) 116c.
[12] G.E. Brown and M. Rho, Phys. Rev. Lett. 66 (1991) 2720.
[13] T. Hatsuda and S. H. Lee, Phys. Rev. C46 (1992) R34.
[14] T. Ullrich et al. (CERES-Collaboration), Nucl. Phys. A610 (1996) 317c.
[15] R. Baur et al. (CERES-Collaboration), Nucl. Inst. Meth. A343 (1994) 87.
[16] R. Brun et al., CERN DD/EE/84-1 (1984), unpublished.
[17] S. V. Afanasiev et al. (NA49-Collaboration), Nucl. Phys. A610 (1996) 188c.
[18] I. G. Bearden et al. (NA44-Collaboration), Nucl. Phys. A610 (1996) 175c.
[19] M. Aggarwal et al. (WA98-Collaboration), Nucl. Phys. A610 (1996) 200c.

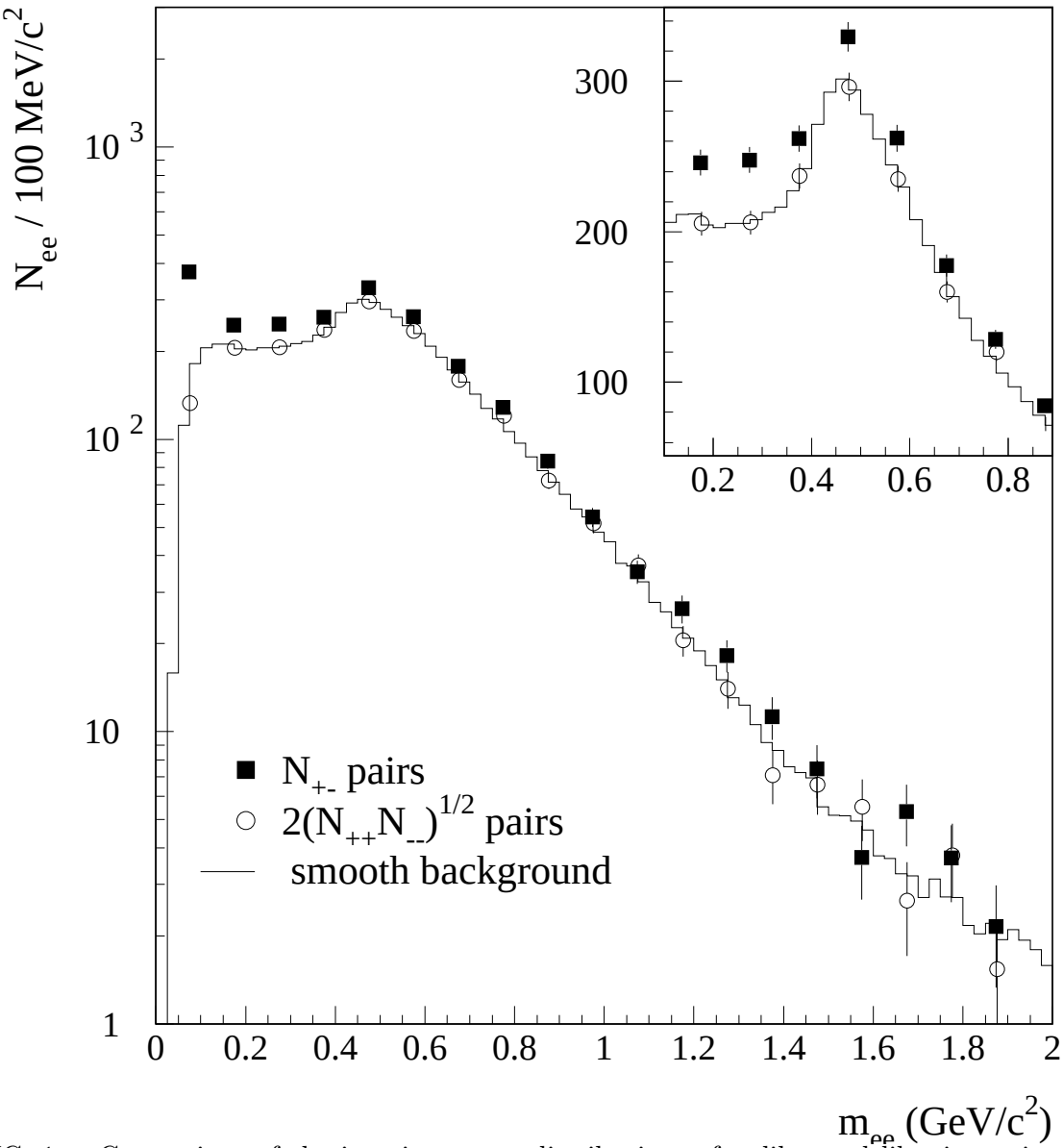

FIG. 1. Comparison of the invariant mass distributions of unlike- and like-sign pairs. The histogram gives the smoothed like-sign spectrum which represents the best estimate of the combinatorial pair background (see text). The insert displays the low-mass region on a linear scale.

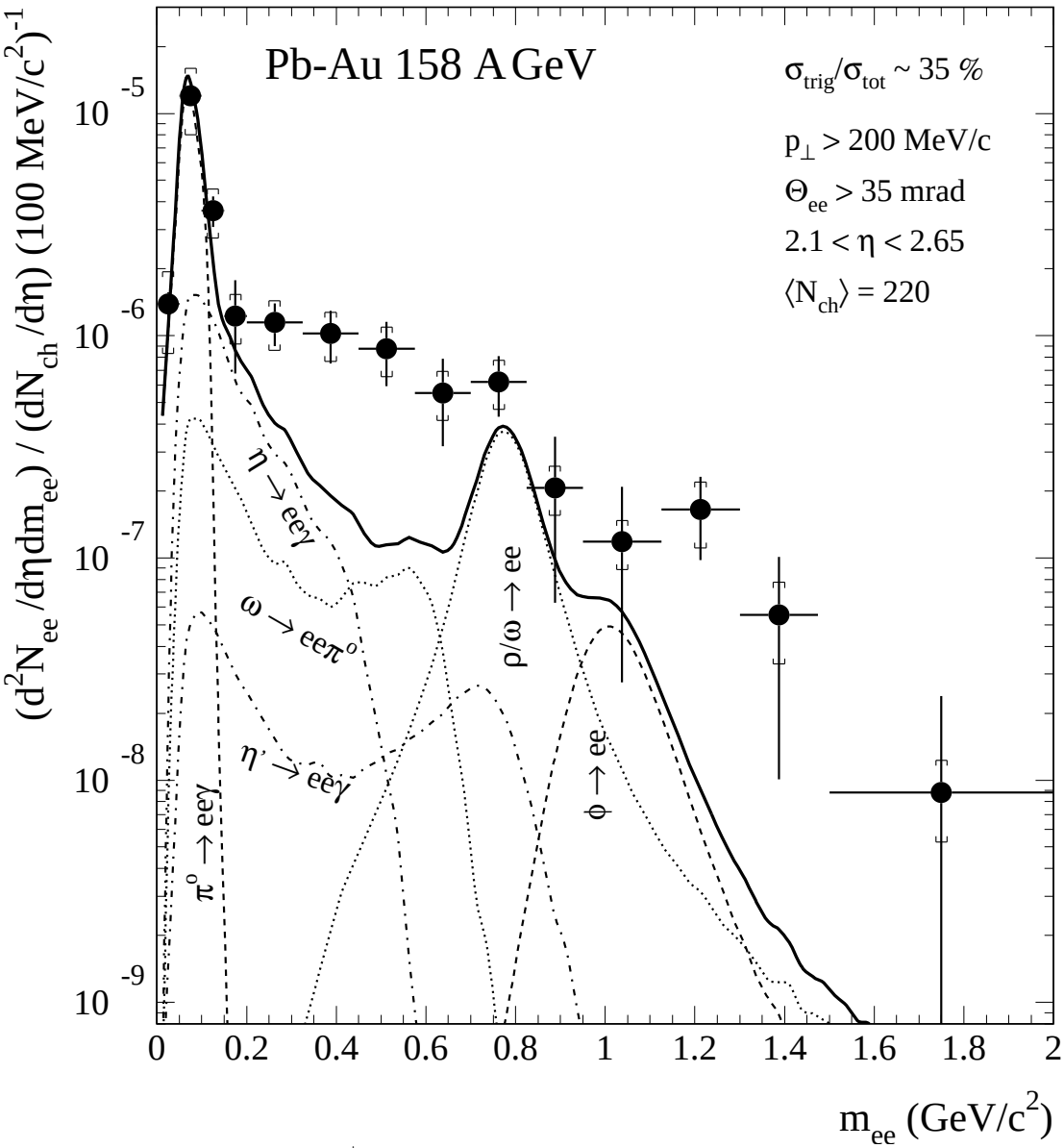

FIG. 2. Inclusive invariant e^+e^- mass spectrum in 158 A GeV Pb-Au collisions normalized to the observed charged-particle density. The statistical errors of the data are shown as bars, the systematic errors are given independently as brackets. The full line represents the e^+e^- yield from hadron decays scaled from p-induced collisions. The contributions of individual decay channels are also shown.

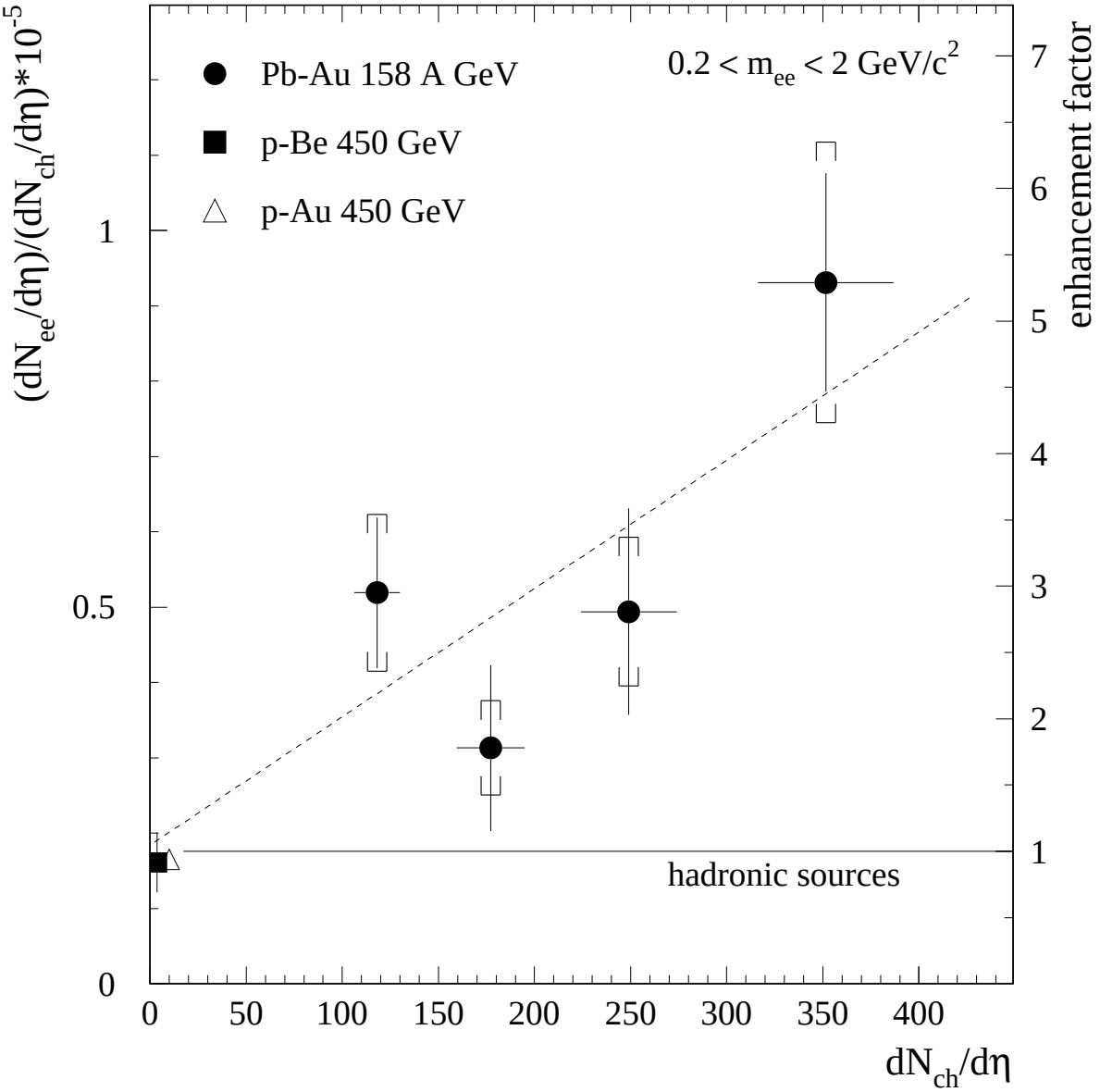

FIG. 3. Multiplicity dependence of the normalized pair yield for Pb-Au collisions. The error on the average multiplicity of each sample is given as horizontal bar. Statistical and systematic uncertainties of the pair yield are shown separately. The dashed line represents a fit to the Pb-Au data assuming a quadratic multiplicity dependence. The solid line shows the expectation from hadronic sources which corresponds to the integral of the contributions shown in Fig. 2. The scale on the right hand side quantifies the enhancement above the expectation from hadron sources. Also shown is the normalized yield measured in p-nucleus collisions [7] .

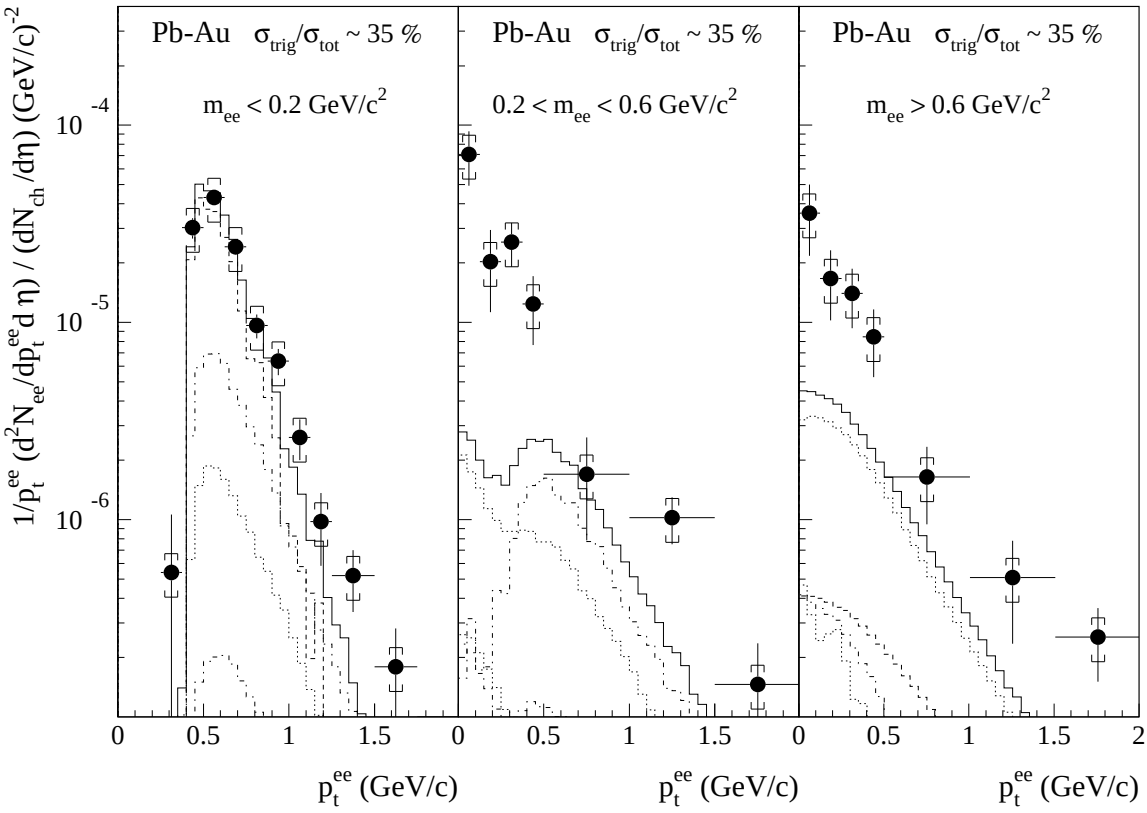

FIG. 4. Inclusive e^+e^- pair $p_\perp$ spectra in 158 GeV/nucleon Pb-Au collisions for three different pair mass ranges. Statistical and systematic errors are given separately. The histograms give the $p_\perp$-distributions expected from individual pardon decay channels and their sum. The normalization of the hadron decay contribution is identical to the one used in Fig.2.